Exploring the *T*–Θ phase diagram of S adsorbed on Au(111) substrate on the Θ = 0.5 ML line

2013 J. Phys.: Condens. Matter 25 045005

(http://iopscience.iop.org/0953-8984/25/4/045005)

J. Phys.: Condens. Matter **25** (2013) 045005 (8pp) doi:10.1088/0953-8984/25/4/045005

Exploring the T–Θ phase diagram of S adsorbed on Au(111) substrate on the $\Theta = 0.5$ ML line

S C Gómez-Carrillo[1] **and P G Bolcatto**[1,2]

[1] Departamento de Física, Facultad de Ingeniería Química, Universidad Nacional del Litoral, Santiago del Estero 2829 S3000AOM Santa Fe, Argentina
[2] Facultad de Humanidades y Ciencias, Universidad Nacional del Litoral, Santa Fe, Argentina

E-mail: scgomez@fiq.unl.edu.ar

Received 10 September 2012, in final form 6 November 2012
Published 12 December 2012
Online at stacks.iop.org/JPhysCM/25/045005

Abstract
Theoretical results for the adsorption of half of a monolayer of S on Au(111) are presented. The simulations were made using a density functional theory (DFT) tight binding approach combined with classical molecular dynamics at 800, 500, 300, 150 and 1 K. By considering a minimal $(2 \times \sqrt{3})$ unit cell, two stable adsorbed phases are found: a dimeric one and another forming a rhomboidal structure depending on the preparation of the sample at high temperatures. Optimized calculations at $T = 0$ K indicate that the stability of the dimeric phase is due to the increase of the binding energies between sulfur atoms. Enforcing previous results (Gómez-Carrillo *et al* 2011 *Phys. Chem. Chem. Phys.* **13** 461) it is verified that at high temperatures ($T > 300$ K) sulfur atoms have a high mobility which allows migration among different adsorption sites. The mobility decreases with the temperature and, as in the previous work, a thermal barrier of 25–30 meV is found. On enlarging the unit cell new agglomerates are found, in good agreement with experimental data.

(Some figures may appear in colour only in the online journal)

1. Introduction

Motivated by the necessity of desulfurization in metal-based catalyzers [1, 2] or by its relevance in atom-size contacts [3, 4], the adsorption of sulfur on noble metals has become a very interesting problem in surface physics. Theoretical and experimental data show that sulfur can be arranged on a Au(111) surface forming commensurate superficial structures or molecular aggregates depending on the coverage and the temperature of the sample [5–10].

Rodriguez *et al* [6], after photoemission and thermal desorption measurements, claimed that for Au(111) surfaces, coverages $\Theta \lesssim 1/3$ ML and temperatures below 300 K, the adsorption is dominated by a single sulfur adatom interacting with gold surface atoms. Further density functional theory (DFT) calculations indicated that the preferred (but not the unique) site of adsorption is the center of a triangle with fcc coordination [6, 11]. In this situation, the sulfur bonds weaken with a trend to accept electrons.

Electrochemical experiments complemented with scanning tunneling microscopy (STM) [5, 7] showed the formation of a $(\sqrt{3} \times \sqrt{3})$R30° superficial phase consistent with a coverage of $\Theta = 1/3$ ML.

Yu *et al* [10], based on low-energy electron diffraction (LEED), STM, normal incidence x-ray standing wavefield absorption (NIXSW) and x-ray photoelectron spectroscopy (XPS) on samples built by evaporation, gave another interpretation of the evolution of adsorption of sulfur at low coverages. While the $(\sqrt{3} \times \sqrt{3})$R30° is the expected phase, its observation in LEED patterns is rare and unstable. Even more interesting is the (5×5) phase, which corresponds to a local $(\sqrt{3} \times \sqrt{3})$R30° sparse arrangement with a (5×5) periodicity. This phase is consistent with a coverage of $\Theta = 0.28$ ML.

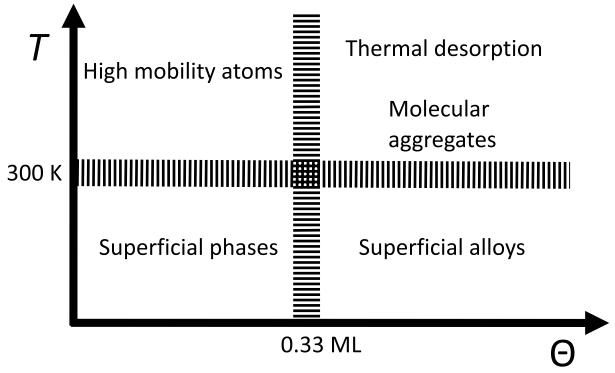

Figure 1. A schematic phase diagram for the adsorption of S on Au(111).

On the other hand, for coverages of $\Theta \gtrsim 1/2$ ML, it is suggested that sulfur atoms form more complex structures which are not easy to characterize geometrically [10], but give early support to the existence of AuS superficial compounds, as was claimed in [8, 9]. However, the measurements in [6] are explained in terms of the occurrence of superficial molecules (S_n ($n = 2, \ldots, 8$)) and particular results, mainly theoretical at $T = 0$ K, indicate the dimerization of adatoms.

By increasing the coverage from $\Theta \gtrsim 1/3$ ML to $\Theta \sim 2/3$ ML, Vericat *et al* [7] showed how the sulfur is aggregated in a mix of $(\sqrt{3} \times \sqrt{3})$R30° with S_3, S_3, $(\sqrt{3} \times \sqrt{3})$R30° plus S_8 and S_8 configurations[3]. For temperatures above 300 K, the S–Au bond is strongly weakened, promoting a high mobility of the adatoms [12], and only some S_n structures can be observed [6, 7] before a thermal desorption process starts.

Summarizing the main experimental and theoretical results on this system, a very schematic T–Θ phase diagram can be drawn (figure 1).

In this paper we explore some features of this phase diagram following the coverage line $\Theta = 1/2$ ML for different temperatures. We find a dimeric phase with energies very close to the monoatomic one, indicating the plausibility of the existence of molecular superstructures at low temperatures. Besides, a previous estimation of the thermal barrier (∼25–30 meV) [12] is reconfirmed and the formation of some kinds of S_n structures are verified when the size of the unit cell is enlarged.

2. Theoretical and numerical methods

The calculations were made in the frame of DFT in its local density approximation (LDA). The FIREBALL [13–16] code, able to calculate systems with translational periodicity, was used. The effects of core electrons and nuclei are incorporated by means of pseudopotentials [17]. The basis sets are (numerical) localized wavefunctions which are strictly equal to zero beyond a cutoff radius r_i ($i = \mathrm{s}, \mathrm{p}, \mathrm{d}$). We selected $r_\mathrm{s} = 4.3a_0$, $r_\mathrm{p} = 4.7a_0$ for sulfur and $r_\mathrm{d} = 4.1a_0$, $r_\mathrm{s} = 4.6a_0$ and $r_\mathrm{p} = 5.2a_0$ for gold, where a_0 is the Bohr radius. The unit cell is composed of four layers of Au, each one with four gold atoms, and two superficial sulfur atoms so that the coverage is $\Theta = 1/2$ ML, as is shown in figure 2. The cell is replicated in the x–y superficial plane, and in the z-direction an empty space of 90 Å (equivalent to ∼ 37 layers) is added in order to simulate the sulfur's superficial effects, but without interaction with the nearest cell along the z-direction. The herringbone reconstruction of the Au(111) surface can be ignored because it is lost when a minimum sulfur coating is added [18, 19].

At temperatures greater than room temperature, sulfur is expected to have a high mobility. Therefore, different geometric configurations can occur depending on the temperature of the sample. To simulate this fact, the system is calculated at 800 K, 500 K, 300 K, 150 K and 1 K. The electronic calculation is complemented with classical molecular dynamics: the atom velocities are assigned randomly following a Maxwell–Boltzmann distribution [14], then the atoms move according to LDA forces and the velocities are rescaled in order to assure a constant kinetic energy (or temperature).

The time step for the simulations is 0.2 fs and a maximum of 16 000 steps are calculated. The tolerance criteria for convergence are 10^{-4} eV/atom for the total energy and 10^{-2} eV Å^{-1} for the forces [12]. In all the cases only the innermost layer of gold is fixed and the three superficial ones plus the adatoms are free to move to optimize the energy. This DFT-MD technique has been successfully used in similar systems exhibiting dynamical fluctuations between two superficial phases [20–22, 12].

Note that the selected time and number of steps do not attempt to reproduce either an experimental cooling or a growth situation. The goal of this selection is to help the system to reach low temperature phases corresponding to local minima of the potential energy, which are not easily predicted from $T = 0$ K calculations.

3. Results and discussion

3.1. LDA plus classical molecular dynamics calculations

Firstly, different geometric configurations compatible with a sample at $T = 800$ K are explored. Hollow-fcc and top locations are adopted as the initial positions for S1 and S2, respectively. Figure 3 shows the positions of the sulfur atoms for each step and the final arrangement for the superficial layer of gold. In figure 3(a1) it is possible to observe how the adsorbates can migrate many times among superficial sites (as a reference, the boiling temperature of S is 717.8 K). The high mobility of the sulfur atoms and the strong displacements of the superficial gold atoms prevent any stabilization in an energy (local) minimum. Several geometric patterns for the adsorbed layer are verified along the simulation. After 16 000 steps of simulation a, dimeric structure is suggested in which the adatoms are placed near bridge (S1) and top (S2) sites. Here, the S–S distance is 2.26 Å. This value is quite close to the equilibrium distance of S_2 in the gas phase, which is 2.06 Å from a FIREBALL calculation [23].

[3] Indeed, in electrochemical experiments the absolute value of the negative electrode potential increases, which implies a step by step reduction of the coverage.

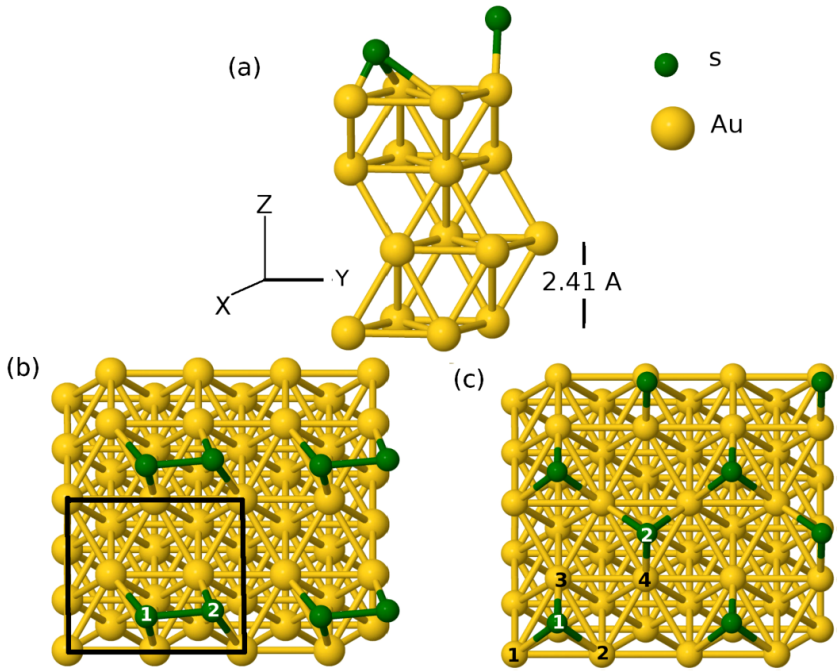

Figure 2. (a) The $(2 \times \sqrt{3})$ unit cell used to simulate a coverage of $\Theta = 1/2$ ML. Gold atoms are located in order to reproduce the correct stacking for this surface. (b), (c) top views of the dimeric and rhomboidal arrangements, respectively. The center of the Au1–Au2–Au3 (Au2–Au3–Au4) triangle is an fcc (hcp) site.

At this point, the system is frozen and the velocities are redefined so that the kinetic energy is compatible with a temperature of 500 K. In figure 3(b1) it is observed that sulfur atoms can jump from site to site but always remain as a dimer.

Subsequent simulations at temperatures of 300, 150 and 1 K, adopting as the initial geometry the final one resulting from the previous temperature, are performed. For 300 K the mobility is lower than that at 500 K (figure 3(c1)) and the adatoms form a very stable dimer.

Finally, for 150 and 1 K, S atoms are not able to jump to different sites and they are stabilized in bridge positions (figure 3(d1)). The impossibility of the adatoms (a dimer in this case) moving to different sites at $T \lesssim 300$ K is in agreement with the result obtained for coverages of $\Theta = 1/3$ ML. In consequence a thermal activation barrier of 25–30 meV can be roughly estimated, in agreement with the corresponding estimation made in [12].

Analyzing the molecular dynamics step by step at 800 K it is observed that after 9000 steps the adatoms are far enough away to outline a rhomboidal phase before the formation of the dimer. Here, the S–S distance is $\simeq$3.7 Å, a distance such that the adatoms have almost no attractive interactions [23]. Then, as a second alternative to explore novel configurations, the calculation is stopped at this point and is restarted for lower temperatures following the same criteria used before. The sequence corresponding to this option is shown in the right panels of figures 3(a2)–(e2).

At 500 K, in spite of the adatoms moving among bridge, hollow and near-top sites, the rhomboidal structure is robust and the relative orientation of the sulfur atoms remains unaltered. Therefore, a commensurate adsorbed superstructure floating over the gold surface occurs. For lower temperatures the rhomboidal structure is located on hollow sites (alternately fcc and hcp ones), although the adatoms are not located exactly at the centers of the triangles (see the discussion of figure 5).

The results introduced in figure 4 reinforce this discussion. In figure 4(a) the evolution of the total energy of the unit cell for the two configurations is presented. Here, the final energy for the dimeric phase is 103 meV lower than for the rhomboidal one. The difference is clearly greater than the numerical error of the calculation ($\simeq$10 meV [12]) although small enough to stabilize any of the two configurations by means of thermal treatment. Regarding the S–S distance (figure 4(b)), the dimer presents minimal (thermal) fluctuations in the range of 2.07–2.51 Å from 500 to 1 K. The fluctuations are always around the equilibrium distance in the adsorbate phase (2.26 Å). Another interesting feature to observe is the evolution of the azimuthal angle; that is, the angle between the x-axis and the line connecting the sulfur atoms S1 and S2 (figure 4(c)). The dimers flip between approximately $-35°$ and $35°$ at 500 K. Indeed, in this case, jumps from site to site mean flipping of the azimuthal angle from negative to positive values. Angles $\sim 0°$ correspond to sulfur atoms on bridge positions; otherwise, one of them goes to (near) an on-top site. At 1 K, the dimeric structure is stabilized with an azimuthal angle of 9° and in a position intermediate between center, bridge and top.

On the other hand, the S–S distance in the rhomboidal arrangement oscillates around its final value of 3.92 Å (figure 4(b)). Besides, the azimuthal angle is always close to 40.9°, which is an indicator of the robustness of this superstructure (figure 4(c)). This geometry corresponds to adsorbates located not on the centers of the gold triangles but

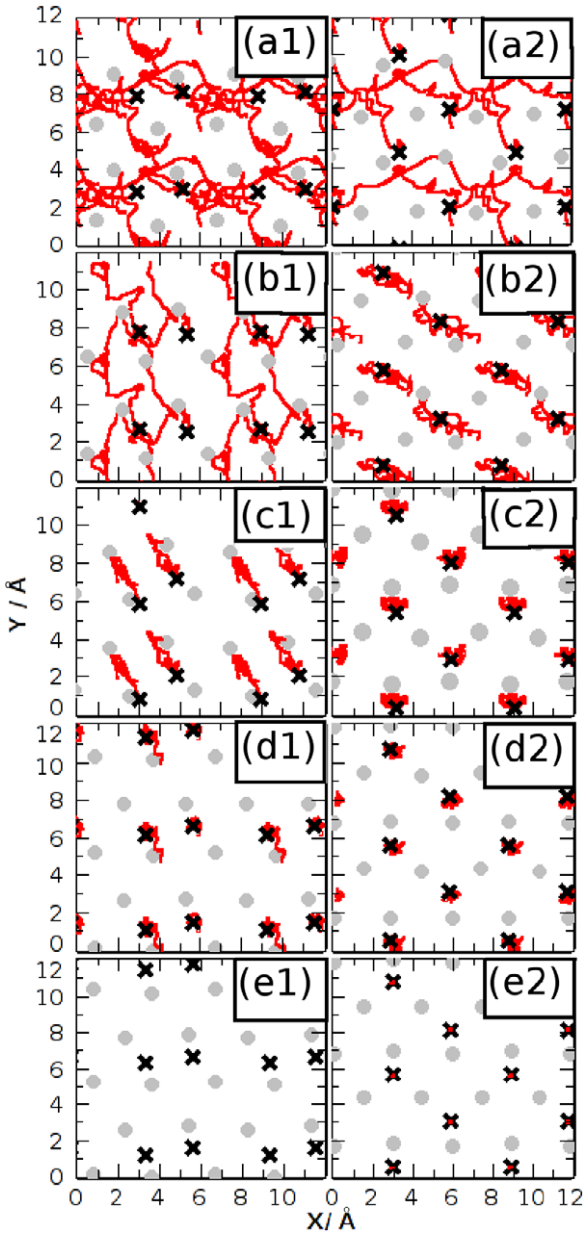

Figure 3. Superficial phases. (a) $T = 800$ K, (b) $T = 500$ K, (c) $T = 300$ K, (d) $T = 150$ K, (e) $T = 1$ K. The left panels correspond to the simulation yielding the dimeric phase and the right panels the rhomboidal one. In all cases the number of simulation steps is 16 000, except in (a2) where only 9000 steps were calculated. The thin (red) lines show the successive positions of the sulfur atoms for each simulation step. The black crosses indicate the final locations of the adatoms after the simulation. The gray points are the final locations of the gold atoms of the outermost layer.

just in the middle of the distance between the horizontal lines connecting surface gold atoms.

3.2. $T = 0$ K calculations

To find the reasons why the dimeric phase is stabilized, additional calculations are performed. The temperature is fixed at 0 K and a full-LDA electronic calculation together with a dynamical quenching for the minimization of energy is started. The dynamical quenching (not molecular dynamics) yields results equivalent to the gradient conjugate scheme [13–16].

Table 1. Differences between the (final) relaxed and crystalline z-positions of the superficial gold atoms. The values are given in Å and the precision is unity on the last digit given. For reference, the distance between (111) planes is 2.41 Å.

	Δz			
	Au1	Au2	Au3	Au4
Dimeric phase				
800 K	0.56	0.71	−0.26	0.42
500 K	0.36	0.12	0.39	0.12
300 K	0.35	0.20	0.12	0.42
150 K	0.13	0.07	0.12	0.19
1 K	0.15	0.04	0.16	0.04
0 K	0.21	−0.01	0.14	−0.24
Rhomboidal phase				
800 K	−0.07	−0.02	0.50	0.96
500 K	0.10	0.85	0.65	−0.33
300 K	0.52	0.39	−0.20	−0.09
150 K	0.51	0.26	−0.12	−0.13
1 K	0.40	0.30	−0.14	−0.12
0 K	0.38	0.39	−0.25	−0.26

Table 2. Distances between the outermost crystalline layers of Au and S atoms. The values are given in Å and the precision is unity on the last digit given. For reference, the distance between (111) planes is 2.41 Å.

	800 K	500 K	300 K	150 K	1 K	0 K
Dimeric phase						
d_{S1-Au}	2.07	2.21	2.56	2.40	2.26	2.09
d_{S2-Au}	2.38	2.47	2.78	2.50	2.24	2.17
Rhomboidal phase						
d_{S1-Au}	2.64	1.86	2.22	1.96	1.96	1.89
d_{S2-Au}	2.65	2.83	2.12	1.91	1.90	1.92

The differences between the crystalline z-positions of the outermost layer of gold and the resulting ones after the simulation are summarized in table 1. While the structure is strongly modified by temperature, the final stabilization at $T = 0$ K gives insight into the influence of the adsorbed layer. For the dimeric phase, the gold atoms labeled by Au1 and Au3 (see figure 2) are corrugated upward; this works as a (minimal) physical barrier that confines the dimers in channels, as is schematically drawn in figure 5. Something similar occurs in the rhomboidal phase: Au1 and Au2 are corrugated upward, pushing the sulfur atoms from the center of the superficial triangle towards near the Au3 and Au4 on-top locations. The geometry of this phase is detailed in figure 5.

Nevertheless, the relaxation is not strong enough to think in terms of formation of superficial gold sulfide (AuS) with 1:1 stoichiometry as is suggested in [8]. In table 2 the z-positions of the sulfur atoms (with respect to the ideal crystalline surface) are shown. In both phases, the sulfur atoms are at ∼2 Å over the surface, that is, a distance 5–10 times greater than the corrugation.

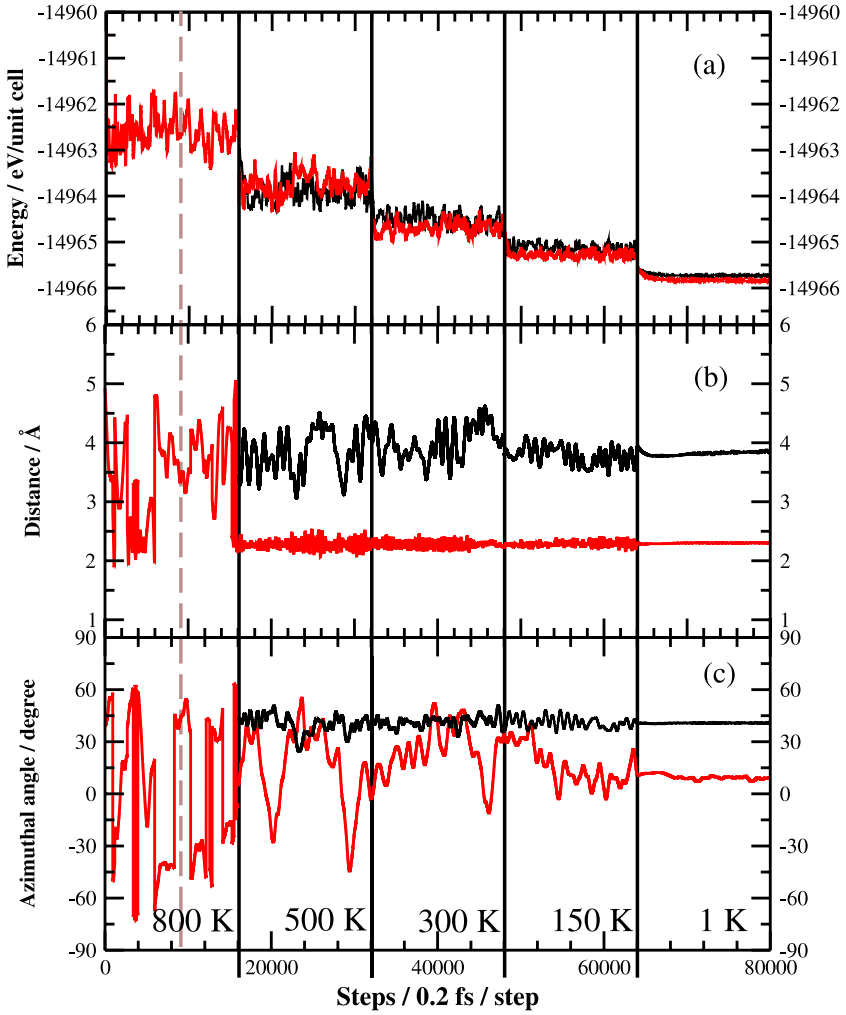

Figure 4. Evolution of (a) the unit cell total energy, (b) the S–S distance and (c) the azimuthal angle measured from the *x*-axis.

By analyzing the energetics in each case it is possible to understand why both phases are stabilized. Table 3 summarizes the relevant energies. In addition to the total energy of the unit cell, the binding energies between S and Au and between S and S are calculated. They are defined as

$$E_{\mathrm{B}}^{\mathrm{S-Au}} = E_{\mathrm{S-Au}} - E_{\mathrm{Au}} - E_{\mathrm{S}} \tag{1}$$

and

$$E_{\mathrm{B}}^{\mathrm{S-S}} = E_{\mathrm{total}} - E_{\mathrm{S1-Au}} - E_{\mathrm{S2-Au}} + E_{\mathrm{Au}}, \tag{2}$$

where $E_{\mathrm{S-Au}}$ is the total energy of a system identical to the converged one in each configuration but with one sulfur adatom extracted. Equivalently, E_{Au} is the total energy of a system identical to the converged one but with two sulfur adatoms extracted. E_{S} is the energy of an isolated sulfur atom.

Moreover, to have a reference for comparison, we calculate the two superficial configurations of the sulfur atoms but with the substrate frozen in the crystalline position.

In the dimeric phase, the relaxation improves the interaction energy between the adatoms and the surface but the phase goes to more stable energies due to the S–S binding energy. On the other hand, the rhomboidal phase gains interaction energy, mainly through the direct binding between individual adsorbates and the relaxed substrate. After Löwdin analysis for the local charge, sulfur species remain with six atomic electrons. Only a slight loss of about 0.05 electrons is verified in all cases.

Table 3. Total and binding energies at $T = 0$ K. The values are given in eV. The (numerical) precision is 10 meV.

	E_{total}	$E_{\mathrm{B}}^{\mathrm{S1-Au}}$	$E_{\mathrm{B}}^{\mathrm{S2-Au}}$	$E_{\mathrm{B}}^{\mathrm{S-S}}$
Dimeric phase				
Crystalline	−14 966.023	−4.478	−4.382	−0.185
Relaxed	−14 966.309	−4.582	−4.553	−0.368
Rhomboidal phase				
Crystalline	−14 965.883	−4.845	−4.929	0.869
Relaxed	−14 966.278	−5.337	−5.156	0.863

3.3. Cluster calculations

To complement the LDA–MD results, a cluster calculation using the GAUSSIAN03 code is performed [24]. The cluster

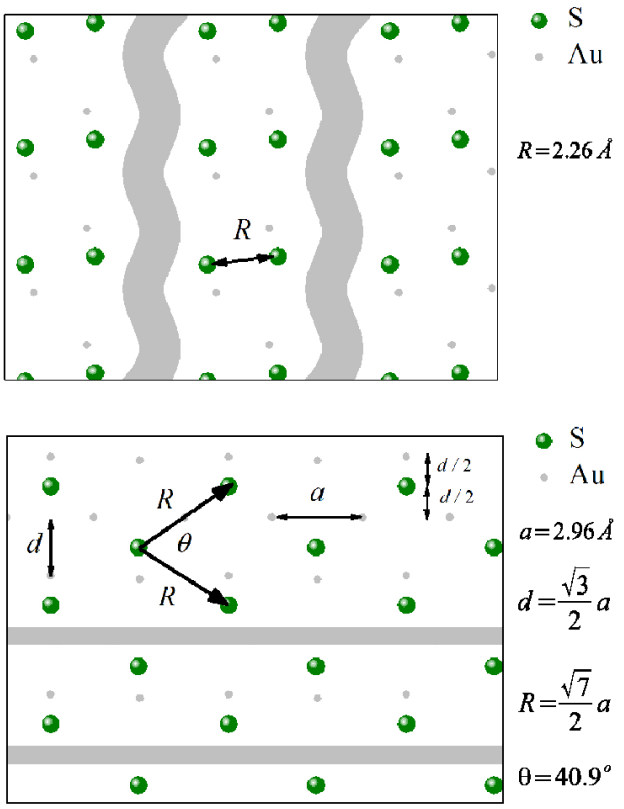

Figure 5. The upper panel shows the dimeric phase and the lower panel shows the rhomboidal phase of $\Theta = 0.5$ ML of S on Au(111) at $T = 0$ K. The gray ribbons indicate the upward corrugation of the superficial gold atoms.

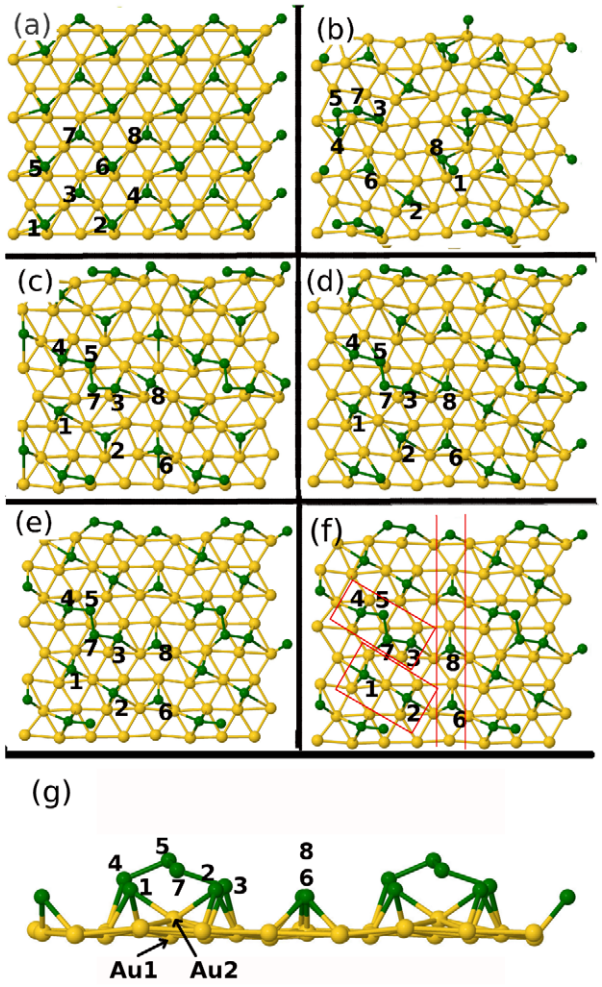

Figure 6. (a) The starting configuration. (b) The final positions for 800 K. (c) The final positions for 500 K. (d) The final positions for 300 K. (e) The final positions for 150 K. (f) The final positions for 1 K. (g) Side view of the final positions of the superficial layer and the adatoms for 1 K.

Table 4. Total energies from cluster calculations. The values are in Hartree.

	LDA	PBE
Dimeric	−2191.175 49	−2188.047 69
Rhomboidal	−2190.867 51	−2187.986 92

is the unit cell optimized from FIREBALL results at $T = 0$ K. One of the aims at this point is to analyze the sensitivity of the results to changes in the exchange–correlation functional, basis set and pseudopotentials. In particular, the LANLDZ atomic basis set [25] and the corresponding pseudopotential are selected. The LANLDZ basis set is able to consider relativistic effects on the gold atoms. Moreover, the system is calculated using the LDA and the Perdew, Burke, Ernzerhof (PBE) functional [26].

The differences between phases are clearly greater for the LDA than the PBE (table 4). However, a quantitative analysis is not appropriate at this point since the geometry of the clusters was not optimized for the basis and functional used in this calculation. The important point here is that, independently of the exchange–correlation functional, the dimeric phase is more stable than the rhomboidal one, in good agreement with the results of the previous sections.

3.4. LDA–MD results on the $2(2 \times \sqrt{3})$ *unit cell*

From the calculations, the possibility of finding molecular aggregates is limited by the size of the unit cell, although increase of the size of the unit cell implies extensive CPU time and other computational resources. As a first attempt to look for new structures, a simulation using a greater unit cell size is presented. Here the $(2 \times \sqrt{3})$ unit cell is duplicated in the x- and y-directions so that it contains four times more atoms than before.

In figure 6 the final positions are shown for the DFT-MD simulations at 800, 500, 300, 150, and 1 K. For 800 K, 8555 steps of simulation were calculated. For the other temperatures, the simulations involved 16 000 steps. In the same way as previous results, the sulfur atoms have a very high mobility at 800 K and they form aggregates of one, two, three and four atoms alternately (figure 6(b)). At 500 K, the system presents three different structures: a double-dimer structure composed of S4–S5 and S3–S7

adatoms, a line of sulfur atoms adsorbed atomically on hollow-fcc sites (S6 and S8 adatoms) and a structure of two fourfold-coordinated sulfur atoms (S1 and S2) sharing a superficial gold atom (Au2) (figure 6(c)). The formation of these molecular superstructures is robust enough to prevent new jumps or superficial reordering at lower temperatures (figures 6(d)–(f)). In other words, the formation of aggregates increases the thermal activation barrier. The lateral view corresponds to the $T = 1$ K final geometry (figure 6(g)).

In the double-dimer structure, the S3 and S4 sulfur atoms are pinned on bridge sites at typical z-distances for S adsorption ($\simeq$2.2 Å). The other atom of the dimer (S7 or S5, respectively) goes up to form a kind of floating dimer (S5–S7) at a greater vertical distance ($\simeq$3.1 Å), but forces an inward corrugation of the Au1 atom of -0.13 Å. The other interesting structure is the one built by S1–Au2–S2 atoms. The natural hollow-fcc adsorption site is moved towards a bridge site mediated by the interaction with the Au2 atom, which is clearly corrugated upward by 0.79 Å(figure 6(g)). This promotion of the Au atom could be a precursor of a superficial alloy, as is claimed in [8, 9], although with a stoichiometry different from 1:1 (AuS). Nevertheless, the coexistence of several structures is in good agreement with the experimental results in [6, 7, 10]. However, the theoretical scenario is not complete yet and more calculations exploring new superficial structures are necessary.

4. Conclusions

Different adsorption situations for $\Theta = 0.5$ ML of S on Au(111) surfaces were explored. The theoretical results—a combination of DFT and MD approaches—indicate the possibility of the occurrence of multiple structures, all of them compatible with previous experimental results. The transformation of S–S_2 on Au(111) for S coverages of 1 and 0.5 ML is suggested in the bibliography data. This coincides with our results which show that a quasi S_2 phase is energetically more stable. We found that this stability is due to the increase in binding energies between S and S. The monoatomic (rhomboidal) phase is stabilized with energies slightly greater than the dimeric phase. In this case the system gains energy because of the strong interaction between the S and one superficial Au. In both cases the mobility of the sulfur atoms at $T \gtrsim 300$ K allows us to estimate a thermal activation energy of 25–30 meV, in the same way as for coverages of $\Theta = 0.33$ ML. When the unit cell is enlarged, new agglomerates are found, in good agreement with experimental data.

Acknowledgments

The authors are supported by the Consejo Nacional de Investigaciones Científicas y Técnicas (CONICET). This work was performed in the frame of grant CAI+D PI-68-344 of the Universidad Nacional del Litoral.

References

[1] Venezia A M, La Parola V, Deganello G, Pawelec B and Fierro J L G 2003 Synergetic effect of gold in Au/Pd catalysts during hydrodesulfurization reactions of model compounds *J. Catal.* **215** 317

[2] Venezia A M, Murania R, Pantaleo G, La Parola V, Scire S and Deganello G 2009 Combined effect of noble metals (Pd, Au) and support properties on HDS activity of Co/SiO_2 catalysts *Appl. Catal. A: Gen.* **353** 296

[3] Ulrich J, Esrail D, Pontius W, Venkataraman L, Millar D and Doerrer L H 2006 Variability of conductance in molecular junctions *J. Phys. Chem.* B **110** 2462

[4] Kiguchi M, Tal O, Wohlthat S, Pauly F, Krieger M, Djukic D, Cuevas J C and van Ruitenbeek J M 2008 Highly conductive molecular junctions based on direct binding of benzene to platinum electrodes *Phys. Rev. Lett.* **101** 046801

[5] Vericat C, Vela M E, Andreasen G, Salvarezza R C, Vázquez L and Martin-Gago J A 2001 Sulfur–substrate interactions in spontaneusly formed sulfur adlayers on Au(111) *Langmuir* **17** 4919

[6] Rodriguez J A, Dvorak J, Jirsak T, Liu G, Hrbek J, Aray Y and González C 2003 Coverage effects and the nature of the metal–sulfur bond in S/Au(111): high-resolution photoemission and density-functional studies *J. Am. Chem. Soc.* **125** 276

[7] Vericat C, Vela M E, Gago J and Salvarezza R C 2004 Sulfur electroadsorption on Au(111) *Electrochim. Acta* **49** 3643

[8] Biener M M, Biener J and Friend C M 2005 Revisiting the S-Au(111) interaction: static or dynamic *Langmuir* **21** 1668

[9] Biener M M, Biener J and Friend C M 2007 Sulfur-induced mobilization of Au surface atoms on Au(111) studied by real-time stm *Surf. Sci.* **601** 1659

[10] Yu M, Ascolani H, Zampieri G, Woodruff D P, Satterley C J, Jones R G and Dhanak V R 2007 The structure of atomic sulfur phases on Au(111) *J. Phys. Chem.* C **111** 10904

[11] Gottschalck J and Hammer B 2002 A density functional theory study of the adsorption of sulfur, mercapto, and methylthiolate on Au(111) *J. Chem. Phys.* **116** 784

[12] Gómez-Carrillo S C and Bolcatto P G 2011 Coexistence of $\sqrt{(3)} \times \sqrt{(3)}$ and quasi linear phases of sulfur adsorbed ($\theta = 1/3$) on a gold(111) substrate *Phys. Chem. Chem. Phys.* **13** 461

[13] Sankey O F and Niklewski D J 1989 *Ab initio* multicenter tight-binding model for molecular-dynamics simulations and other applications in covalent systems *Phys. Rev.* B **40** 3979

[14] Demkov A A, Ortega J, Sankey O F and Grumbach M P 1995 Electronic structure approach for complex silicas *Phys. Rev.* B **52** 1618

[15] Lewis J P, Glaesemann K R, Voth G A, Fritsch J, Demkov A A, Ortega J and Sankey O F 2001 Further developments in the local-orbital density-functional-theory tigh-binding method *Phys. Rev.* B **64** 195103

[16] Jelínek P, Wang H, Lewis J P, Sankey O F and Ortega J 2005 Multicenter approach to the exchange–correlation interactions in *ab initio* tight-binding methods *Phys. Rev.* B **71** 235101

[17] Hamann D R 1989 Generalized norm-conserving pseudopotentials *Phys. Rev.* B **40** 2980

[18] Woll Ch, Chiang S, Wilson R J and Lippel P H 1989 *Phys. Rev.* B **39** 7988

[19] Barth J V, Schuster R, Behm R J and Ertl G 1996 *Surf. Sci.* **348** 280

[20] Avila J, Mascaraque A, Michel E G, Asensio M C, LeLay G, Ortega J, Pérez R and Flores F 1999 Dynamical fluctuations as the origin of a surface phase transition in Sn/Ge(111) *Phys. Rev. Lett.* **82** 442

[21] Farías D, Kaminski W, Lobo J, Ortega J, Hulpke E, Pérez R, Flores F and Michel E G 2003 Phonon softening, chaotic motion and order disorder transition in Sn/Ge(111) *Phys. Rev. Lett.* **91** 016103

[22] González C, Flores F and Ortega J 2006 Soft phonon, dynamical fluctuations, and a reversible phase transition: indium chains on silicon *Phys. Rev. Lett.* **96** 136101

[23] Gómez-Carrillo S C and Bolcatto P G 2012 Sulfur adsorbed ($\theta = 1/2$) on gold(111) substrate *J. Supercond. Nov. Magn.* at press

[24] Frisch M J *et al* 2005 *Gaussian 03, revision E.01* (Wallingford, CT: Gaussian)

[25] Hay P J and Wadt W R 1985 *Ab initio* effective core potentials for molecular calculations. potentials for the transition metal atoms Sc to Hg *J. Chem. Phys.* **82** 270

[26] Perdew J P, Burke K and Ernzerhof M 1996 Generalized gradient approximation made simple *Phys. Rev. Lett.* **77** 3865